
*Short Review***Magnéli oxides as promising *n*-type thermoelectrics****Gregor Kieslich,^{1*} and Wolfgang Tremel^{2*}**¹ Functional Inorganic and Hybrid Materials Group, Department of Materials Science and Metallurgy, University of Cambridge, 27 Charles Babbage Road, Cambridge CB3 0FS, UK² Institut für Anorganische Chemie und Analytische Chemie der Johannes Gutenberg-Universität, Duesbergweg 10-14, D-55099 Mainz, Germany* **Correspondence:** Email: gk354@cam.ac.uk, tremel@uni-mainz.de

Abstract: The discovery of a large thermopower in cobalt oxides in 1997 lead to a surge of interest in oxides for thermoelectric application. Whereas conversion efficiencies of *p*-type oxides can compete with non-oxide materials, *n*-type oxides show significantly lower thermoelectric performances. In this context so-called Magnéli oxides have recently gained attention as promising *n*-type thermoelectrics. A combination of crystallographic shear and intrinsic disorder lead to relatively low thermal conductivities and metallic-like electrical conductivities in Magnéli oxides. Current peak-*zT* values of 0.3 around 1100 K for titanium and tungsten Magnéli oxides are encouraging for future research. Here, we put Magnéli oxides into context of *n*-type oxide thermoelectrics and give a perspective where future research can bring us.

1. Introduction

In the complex energy landscape of the future the materials choice in application oriented technologies is of particular importance and the materials must fulfill today's sustainability criteria such as high abundance, low toxicity and long-term stability. Oxide based materials usually fulfill all criteria and consequently they attracted a lot of interest in context of thermoelectric research [1,2,3]. In addition, oxides take advantage of low-cost and scalable preparation techniques such as consolidation and simultaneous preparation using spark plasma sintering [4,5]. On the other hand, the primarily ionic metal-oxygen bond lead to unfavorable intrinsic properties of oxides that makes an optimization of their thermoelectric properties particularly challenging. Therefore it is not surprising that current state of the art materials are non-oxide materials, for example lead and bismuth tellurides [6], silicides [7], and Zintl compounds [8]. However, the discovery of a large thermopower in cobalt oxides more than 15 years ago [9] has triggered a surge of interest, and today a few oxide materials are known that exhibit fascinating thermoelectric properties.

In general, in thermoelectrics the ultimate goal is the maximization of the thermoelectric figure of merit $zT = (\alpha^2\sigma/\kappa) \cdot T$ with α being the thermopower, σ the electrical conductivity, κ the thermal conductivity and T the absolute temperature. The interrelation of the different parameters makes an optimization for all kind of materials difficult, however, today different approaches are known to decouple material properties for example, the introduction of crystalline interfaces on different length scales which (i) decrease the thermal conductivity due to grain boundary scattering and further (ii) introduce electron filtering mechanisms [10,11].

Among the many available oxide materials, layered *p*-type conductors exhibit the best thermoelectric performances with zT values of 1.4 at 1000 K ($\text{Bi}_{1-x}\text{Ba}_x\text{CuSeO}$) and 1.2 at 873 K ($\text{Ca}_3\text{Co}_4\text{O}_9$) [3,12]. Their good performances originate from high carrier mobilities within the layers and relatively low thermal conductivities. Nowadays, there is a gap in the thermoelectric performance between *n*-type and *p*-type materials, the latter showing superior properties that must be closed for wide commercialization of oxide-based thermogenerators. Current state of the art *n*-type oxide materials, which have been studied intensively during the past decade, include co-doped zinc oxides, indium tin oxides and strontium titanates. Although thermoelectric performances of *n*-type materials were steadily enhanced, today, only a few reports exist with zT values of 0.6 ($\text{Zn}_{0.96}\text{Al}_{0.02}\text{Ga}_{0.02}\text{O}$ at 1273 K) and 0.45 ($\text{In}_{1.8}\text{Ge}_{0.2}\text{O}_3$ at 1273 K) [13,14].

2. Crystallographic shear in Magnéli oxides

The reduction of transition metal oxides such as TiO_2 , V_2O_5 , MoO_3 and WO_3 , either with the corresponding metal or by hydrogen gas, leads to the introduction of crystallographic shear (CS) planes as structure motif, see Figure 1a [18]. Within the crystal structure the coordination of the metal cation remains basically unchanged and the anion coordination number is increased to accommodate the reduced metal to oxygen ratio. In case of a ReO_3 -like parent structure, for example MO_3 ($\text{M} = \text{Mo}^{6+}$, W^{6+}), the reorganization leads to the introduction of planes where MO_6 octahedra are now edge-shared, so-called CS planes. In titanium oxides, which adopt the rutile-type as parent structure, face-sharing octahedra are introduced. Regarding the mechanism, the formation of CS planes starts with a perfect crystal and oxygen vacancies are introduced either by heating or chemical reduction. These vacancies emerge at the crystal surface and then diffuse to certain planes within the crystal where the energy of the vacant sites is minimized. In the last step, these vacancies are then eliminated by the introduction of corner/face sharing octahedra, the so-called crystallographic shear planes. A similar ordering mechanism of vacant sites is encountered in Fe_{1-x}S and Fe_{1-x}O compounds where the reduction of Coulomb interactions is the driving force [21]. Before A. Magnéli discovered the first homologous series of $\text{Ti}_n\text{O}_{2n-1}$ and $\text{W}_n\text{O}_{3n-2}$ in the 1950's [15,16] compounds such as $\text{TiO}_{1.90}$, $\text{MoO}_{2.75}$ and $\text{WO}_{2.90}$ were believed to be nonstoichiometric with a wide homogeneity range. Since then, electron imaging and diffraction techniques confirmed the proposed structural concept, and today many different homologous series including non-equilibrium structures have been discovered for many early transition metal oxides [17,18].

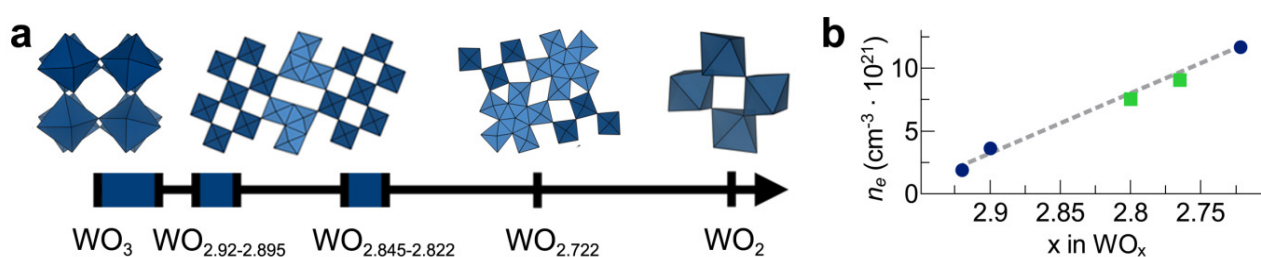


Figure 1. (a) Structure motifs in the quasi ternary system $\text{WO}_3\text{-WO}_2$ and (b) the corresponding carrier concentration (blue = experiment, green = theory; data adapted from Reference 18). Crystallographic shear planes lying on $\{102\}$ planes and $\{103\}$ planes are observed between $0.005 < x < 0.155$. For larger values of x pentagonal columns are the dominating structure motif, as observed for $\text{WO}_{2.833}$ ($\text{W}_{24}\text{O}_{68}$) and $\text{WO}_{2.722}$ ($\text{W}_{18}\text{O}_{49}$) [19].

The introduction of CS planes is associated with a partial reduction of the metal centers. The electrons are available in d orbitals of the reduced metal centers and lead to n -type conduction. In order to understand the electronic structure in more detail, the nature of the partially filled d orbitals must be considered which crucially depends on the underlying crystal structure [22]. In general, with increasing reduction more charge carriers are introduced in the system as shown in Figure 1b for $\text{WO}_3\text{-WO}_2$ [19]. Therefore the carrier concentration, and in turn the electronic transport properties, can be altered by extent of reduction [23,24,25]. It is interesting to note that Magnéli oxides show a certain cycling stability of the physical properties as further oxygen loss is a known issue for most oxides at high temperatures. Detailed thermal stability studies on reactive sputtered tungsten oxide coatings reveal no phase transformations up to a temperature of 923 K [26]. However, at this stage of research it is crucial to focus at fundamental property-relationships rather than on device related issues.

3. Thermoelectric properties of Magnéli oxides

The thermoelectric properties of Magnéli oxides are strongly related to the CS plane density and accompanied charge carrier concentration. In 2010, Harada et al. investigated the high temperature thermoelectric properties of titanium oxides which belong to the homologues series $\text{Ti}_n\text{O}_{2n-1}$ ($n = 2, 3, \dots$), and they explored the influence of CS planes on the thermal conductivities [28]. They concluded that CS planes in combination with their intrinsic disorder are effective scattering centers for phonons, which we demonstrated for tungsten Magnéli phases shortly after [25]. In general, bulk titanium and tungsten Magnéli oxides show thermal conductivities between 2 and $4 \text{ Wm}^{-1}\text{K}^{-1}$ over the whole temperature range. Structural engineering, for example the use of inclusions on different length scales or the preparation of bulk-nano composite materials, further decreased the thermal conductivity of Magnéli oxides to $\kappa \sim 2 \text{ Wm}^{-1}\text{K}^{-1}$ [28,29,30]. Although the observed thermal conductivities are relatively low for oxide materials, oxyselenides show that there might be still room for improvements available ($\text{Bi}_{1-x}\text{BaCuSeO}$, $\kappa = 0.4\text{--}0.8 \text{ Wm}^{-1}\text{K}^{-1}$) [30]. In particular, by applying a random-walk energy model [31] the amorphous (lower) limit of the thermal conductivity is

calculated to $\sim 1\text{--}1.5 \text{ Wm}^{-1}\text{K}^{-1}$ for Magnéli oxides which would further enhance thermoelectric performances.

Looking at the electronic transport properties, the conduction mechanism seems to vary with the extent of reduction. Whereas a clear metallic behavior was observed for highly reduced compounds such as polycrystalline $\text{WO}_{2.722}$ ($\rho_{300\text{K}} \sim 0.1 \text{ m}\Omega\text{cm}$), polaron conduction with very low activation energies around 0.05 eV was found for less reduced compounds [24,32]. However, in a data-mining study, Gaultois et al. found a threshold electrical conductivity of approx. $\rho < 10 \text{ m}\Omega\text{cm}$ that all high- zT materials obey [33]. Such metallic materials are supposed to have low Seebeck coefficients, notwithstanding almost all high-performance thermoelectric materials violate this principle. For example, Na_xCoO_2 is metallic and the spin contribution to thermopower (or arguably, the unique band structure) lead to a unexpected high Seebeck coefficient ($\alpha_{300\text{K}} = 100 \mu\text{V/K}$) and low electrical resistivity ($\rho_{300\text{K}} = 0.2 \text{ m}\Omega\text{cm}$) [34]. Following the idea of spin contribution, the thermopower in polaron conductors is the available entropy (or energy) per carrier and indeed, the experimental results [35] for Magnéli oxides are in agreement with Heike's formula [36]. In general titanium oxides with thermopowers between $100\text{--}150 \mu\text{VK}^{-1}$ ($\text{Ti}_n\text{O}_{2n-1}$, $n = 4, 5, 6, 8$) show higher absolute Seebeck values than tungsten oxides $50\text{--}80 \mu\text{VK}^{-1}$ ($\text{W}_{20}\text{O}_{58}$) [27,28,35,38]. Note, that the properties strongly vary with the applied preparation technique due to the high intrinsic disorder and often mixtures of Magnéli oxides are characterized. This issue was earlier addressed by Tilley et al. who showed that in ampoule reactions the thermodynamic equilibrium state of Magnéli oxides is rarely achieved [20]. Present approaches, such as spark plasma sintering, lead to phase pure materials, however, diffraction domains are usually below 1 micron and show a high amount of structural disorder and strain [29]. Therefore, a detailed phase analysis with (synchrotron) PXRD techniques in combination with SEM and (HR) TEM investigations is essential. Today, the observed transport properties in Magnéli oxides result in peak- zT values of 0.3–0.4 at 1100 K for nitrogen doped titanium oxides and SPS-processed TiO_{2-x} nanoparticles [28,38]. An overview of current figure of merits in comparison with other n -type oxide materials is given in Figure 2.

So far, thermoelectric studies on Magnéli oxides rather have focused on structural engineering than on optimizing electronic transport properties. Consequently, bulk-nano Magnéli composite materials were identified to exhibit enhanced thermal transport properties due to interfacial phonon scattering. The natural next step towards improved thermoelectric performances is the optimization of electronic transport properties. Here, particularly interesting is the optimization of the charge carrier concentration towards an optimized power-factor. For tungsten Magnéli oxides, the optimal charge carrier concentration seems to be around $10^{20}\text{--}10^{21} \text{ carrierscm}^{-3}$ which corresponds to slightly oxidized $\text{W}_{20}\text{O}_{58}$. Since the thermoelectric figure is a combination of thermal and electronic transport properties, significant improvements are expected in upcoming years which are driven by improved electronic transport properties. In the high temperature regime ($T > 1200 \text{ K}$), zT values of 0.6 seem to be easily accessible and in case powerful methodologies towards enhanced electronic properties will be discovered even larger values are expected which makes Magnéli oxides an interesting family for thermoelectrics.

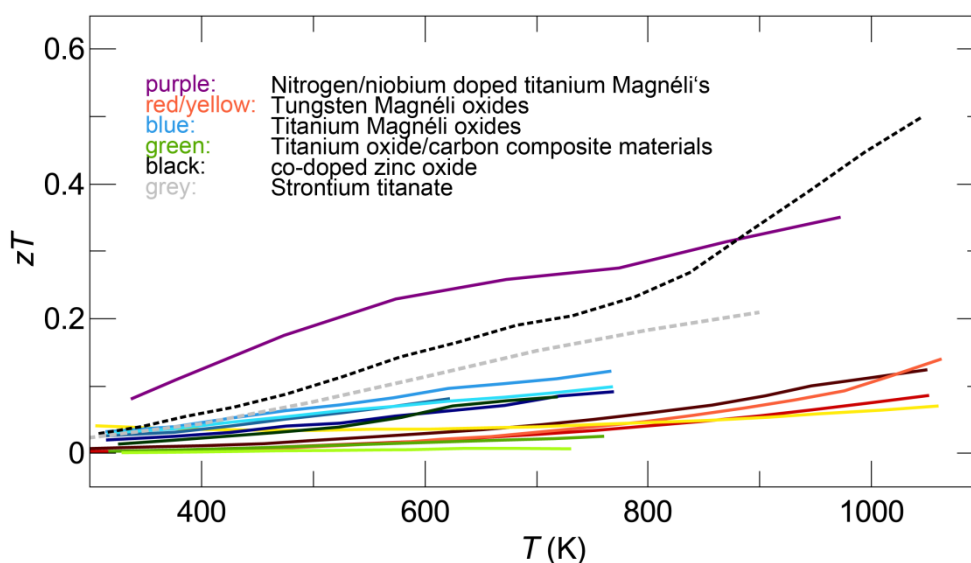


Figure 2. Overview of thermoelectric figures of merit of n -type Magnéli oxides in comparison with strontium titanate (containing yttrium stabilized zirconia nano-inclusions, YSZ) and co-doped zinc oxide. zT values were adapted from the literature, see references [4,14,25,27–29,35,37,38,40]. Note, zinc oxides have been investigated for a long time as n -type thermoelectric oxides but only a few reports exist that report zT values larger than 0.4.

Acknowledgments

The authors acknowledge support from the DFG priority program SPP1386 Nanostructured Thermoelectrics. G.K. is the holder of a postdoctoral fellowship granted by the Deutsche Forschungsgemeinschaft (www.dfg.de/en), KI1879.

References

1. Gaultois MW, Sparks TD, Borg CKH, et al. (2013) Data-Driven Review of Thermoelectric Materials: Performance and Resource Considerations. *Chem Mater* 15: 2911–2920.
2. He J, Liu Y, Funahashi R (2011) Oxide thermoelectrics: The challenges, progress, and outlook. *J Mater Res* 15: 1762–1772.
3. Nag A, Shubha V (2014) Oxide Thermoelectric Materials: A Structure–Property Relationship. *J Elec Mater* 4: 962–977.
4. Kieslich G, Birkel CS, Douglas JE, et al. (2013) SPS-assisted preparation of the Magnéli phase $\text{WO}_{2.90}$ for thermoelectric applications. *J Mater Chem A* 42: 13050–13054.
5. Veremchuk I, Antonyshyn I, Candolfi C, et al. (2013) Diffusion-Controlled Formation of Ti_2O_3 during Spark-Plasma Synthesis. *Inorg Chem* 52:4458–4463.
6. Biswas K, He J, Blum ID, et al. (2012) High-performance bulk thermoelectrics with all-scale hierarchical architectures. *Nature* 489: 414–418.
7. Mingo N, Hauser D, Kobayashi NP, et al. (2009) “Nanoparticle-in-Alloy” Approach to Efficient Thermoelectrics: Silicides in SiGe. *Nano Lett* 2: 711–715.

8. Toberer ES, May AF, Snyder GJ (2010) Zintl Chemistry for Designing High Efficiency Thermoelectric Materials. *Chem Mater* 3: 624–634.
9. Terasaki I, Sasago Y, Uchinokura K (1997) Large thermoelectric power in NaCo_2O_4 single crystals. *Phys Rev B* 20: R12685.
10. Heremans JP, Dresselhaus MS, Bell LE, et al. (2013) When thermoelectrics reached the nanoscale. *Nature Nanotechnol* 7: 471–473.
11. Zebarjadi M, Esfarjani K, Shakouri A, et al. (2009) Effect of Nanoparticles on Electron and Thermoelectric Transport. *J Elec Mater* 7: 954–959.
12. Zhao L, He J, Berardan D, et al. (2014) BiCuSeO oxyselenides: new promising thermoelectric materials. *Energy Env Sci* 7: 2900–2924.
13. Bérardan D, Guilmeau E, Maignan A, et al. (2008) $\text{In}_2\text{O}_3\text{:Ge}$, a promising n-type thermoelectric oxide composite. *Solid State Comm* 1-2: 97–101.
14. Ohtaki M, Araki K, Yamamoto K (2009) High Thermoelectric Performance of Dually Doped ZnO Ceramics. *J Elec Mater* 7: 1234–1238.
15. Andersson S, Collén B, Kuylenstierna U, et al. (1957) Phase Analysis Studies on the Titanium-Oxygen System. *Acta Chem Scand* 11: 1641–1652.
16. Gadó P, Magnéli A, Niklasson RJV, et al. (1965) Shear Structure of the Wolfram Oxide $\text{WO}_{2.95}$. *Acta Chem Scand* 19: 1514–1515.
17. Bursill LA, Hyde BG (1971) Crystal structures in the $\{132\}$ CS family of higher titanium oxides $\text{Ti}_n\text{O}_{2n-1}$. *Acta Cryst B* 1: 210–215.
18. Eyring LR, Tai LT (1973) The Structural Chemistry of Extended Defects. *Annu Rev Phys Chem* 1: 189–206.
19. Migas DB, Shaposhnikov VL, Borisenko VE (2010) Tungsten oxides. II. The metallic nature of Magnéli phases. *J Appl Phys* 9: 93714.
20. Booth J, Ekström T, Iguchi E, et al. (1982) Notes on phases occurring in the binary tungsten-oxygen system. *J Solid State Chem* 3: 293–307.
21. Kelm K, Mader W (2006) The Symmetry of Ordered Cubic $\gamma\text{-Fe}_2\text{O}_3$ investigated by TEM. *Z. Naturforsch B* 61b: 665–671.
22. Canadell E, Whangbo MH (1991) Conceptual aspects of structure-property correlations and electronic instabilities, with applications to low-dimensional transition-metal oxides. *Chem Rev* 5: 965–1034.
23. Bartholomew R, Frankl D (1969) Electrical Properties of Some Titanium Oxides. *Phys Rev* 3: 828–833.
24. Sahle W, Nygren M (1983) Electrical conductivity and high resolution electron microscopy studies of WO_{3-x} crystals with $0 \leq x \leq 0.28$. *J Solid State Chem* 2: 154–160.
25. Kieslich G, Veremchuk I, Antonyshyn I, et al. (2013) Using crystallographic shear to reduce lattice thermal conductivity: high temperature thermoelectric characterization of the spark plasma sintered Magnéli phases $\text{WO}_{2.90}$ and $\text{WO}_{2.722}$. *Phys Chem Chem Phys* 37: 15399–15403.
26. Parreira NMG, Polcar T, Caalerio A (2007) Thermal stability of reactive sputtered tungsten oxide coatings. *Surface and Coatings Technol* 201: 7076–7082.
27. Harada S, Tanaka K, Inui H, (2010) Thermoelectric properties and crystallographic shear structures in titanium oxides of the Magnéli phases. *J Appl Phys* 8: 83703–83709.
28. Mikami M, Ozaki K, (2012) Thermoelectric properties of nitrogen-doped TiO_{2-x} compounds. *J Phys Conf Ser* 379: 12006–12012.

29. Kieslich G, Burkhardt U, Birkel CS, et al. (2014) Enhanced thermoelectric properties of the n-type Magnéli phase $\text{WO}_{2.90}$: Reduced thermal conductivity through microstructure engineering. *J Mater Chem A* 2: 13492–13497.
30. Li J, Sui J, Pei Y, et al. (2012) A high thermoelectric figure of merit $ZT > 1$ in Ba heavily doped BiCuSeO oxyselenides. *Energ Environ Sci* 9: 8543–8547.
31. Cahill DG, Watson SK, Pohl RO (1992) Lower limit to the thermal conductivity of disordered crystals. *Phys Rev B* 46: 6131–6140.
32. Goodenough J (1970) Interpretation of $\text{M}_x\text{V}_2\text{O}_{5-\beta}$ and $\text{M}_x\text{V}_{2-y}\text{T}_y\text{O}_{5-\beta}$ phases. *J Solid State Comm* 3-4: 349–358.
33. Gaultois MW, Sparks TD, Borg CKH, et al. (2013) Data-Driven Review of Thermoelectric Materials: Performance and Resource Considerations. *Chem Mater* 25: 2911–2920.
34. Hebert S, Maignan A (2010) Thermoelectric Oxides, In: Bruce DW, O'Hare Dermot, Walton RI, Functional Oxides, 1 Eds, West Sussex, John Wiley & Sons, 203–255.
35. Backhaus-Ricoult M, Rustad JR, Vargheese D, et al. (2012) Levers for Thermoelectric Properties in Titania-Based Ceramics. *J Elec Mater* 6: 1636–1647.
36. Chaikin P, Beni G (1976) Thermopower in the correlated hopping regime. *Phys Rev B* 2: 647–651.
37. Liu C, Miao L, Zhou J, et al. (2013) Chemical Tuning of TiO_2 Nanoparticles and Sintered Compacts for Enhanced Thermoelectric Properties. *J Phys Chem C* 22: 11487–11497.
38. Fuda K, Shoji T, Kikuchi S, et al. (2013) Fabrication of Titanium Oxide-Based Composites by Reactive SPS Sintering and Their Thermoelectric Properties. *J Elec Mater* 7: 2209–2213
39. Wang N, Chen H, He H, et al. (2013) Enhanced thermoelectric performance of Nb-doped SrTiO_3 by nano-inclusion with low thermal conductivity. *Sci Reports* 3: 3449–3453.
40. Portehault D, Maneeratana V, Candolfi C, et al. (2011) Facile General Route toward Tunable Magnéli Nanostructures and Their Use As Thermoelectric Metal Oxide/Carbon Nanocomposites. *ACS Nano* 5: 9052–9061.

© 2014, Gregor Kieslich, et al. licensee AIMS Press. This is an open access article distributed under the terms of the Creative Commons Attribution License (<http://creativecommons.org/licenses/by/4.0>)